Size effect of the parallel-plate geometry on the rheological behavior of bentonite suspensions

Yuan Lin, Wei Wang, Hai Zhu, Jiawang Chen, Nhan Phan-Thien, and Dingyi Pan

Citation: Journal of Rheology **64**, 111 (2020); doi: 10.1122/1.5116118
View online: https://doi.org/10.1122/1.5116118
View Table of Contents: https://sor.scitation.org/toc/jor/64/1
Published by the The Society of Rheology

Size effect of the parallel-plate geometry on the rheological behavior of bentonite suspensions

Yuan Lin,[1] Wei Wang,[1] Hai Zhu,[1] Jiawang Chen,[1,a)] Nhan Phan-Thien,[2] and Dingyi Pan[3]

[1]*Institute of Ocean Engineering and Technology, Ocean College, Zhejiang University, Zhoushan 316021, China*
[2]*Department of Mechanical Engineering, National University of Singapore, Singapore 117576, Singapore*
[3]*Department of Engineering Mechanics, Zhejiang University, Hangzhou 310027, China*

(Received 21 June 2019; final revision received 25 November 2019; published 17 December 2019)

Abstract

The change of the rheological behavior of a bentonite suspension with the gap of the parallel-plate geometry in a rotational rheometer is investigated. An obvious gap-dependent behavior is found in both the gel and flowing states, based on which it is found that slip at the boundary plays an important role in the viscometric measurement at low shear rates, as well as in the small amplitude oscillatory shear experiment; shear banding is considered to take place at the vicinity of the yielding point, as well as in flows at low shear rates if the boundary slip is suppressed by using rough plates. Furthermore, relaxation behavior, similar to that of a polymeric system, is observed. The motion of the gel structure is slower with increasing gap, indicating a larger size of the networking structure. This is also the origin for the decrease of the yield stress observed with increasing gap. © *2019 The Society of Rheology.* https://doi.org/10.1122/1.5116118

I. INTRODUCTION

Clay sediments are main components of the deep-sea sediment [1], and their rheological properties are determined by the strong interactions between suspended clay particles in water. Therefore, a better understanding of the flowing behavior of clay suspensions is important in any technical deep-sea activity, in assessing loading on immersed infrastructures, etc. Clay particles are disk-shaped with their faces carrying permanently negative charges. Their edges are positively charged in an acidic condition, while negatively charged in an alkaline condition. As a result, strong interparticle electrostatic interactions are expected, which complicates the rheological behavior [2–12]. Due to the face-to-face and face-to-edge interactions, clay platelets aggregate to form a network structure, allowing gelation to take place. Therefore, depending on the clay minerals used, at a low ionic strength, and above a critical clay concentration (i.e., the gel point), the system may be solidlike at the static state (gel state), while it becomes fluidlike when a shear stress larger than a critical stress (the yield stress) is applied. With increasing shear rate or stress, the viscosity decreases significantly, approaching a constant value at a high level of shearing.

At the gel state, the yield stress, τ_y, is considered as one of the most important rheological properties. τ_y is mainly related to the electrostatic potential of the charged platelets, which is from either the face-edge attractive interaction [13–15] or the face-face repulsive interaction [12,16,17]. Leong *et al.* [18] find with cryo-SEM measurements on sodium montmorillonite samples that clay platelets bend with curling edges, to facilitate overlapping face-edge attractive interactions, and the face-face repulsive forces regulate the microstructure, resulting in an open cellular spongelike microstructure. Factors such as *p*H, the ionic strength, and the clay concentration could easily change the yield behavior. On the other hand, in the flowing state, Pignon *et al.* [10] observe a deformation and a disaggregation of the gel structure, from the microscale to the nanoscale range with increasing shear. Paineau *et al.* [2] find an orientation of the platelets, aligning with the flow to reduce the suspension viscosity. At high shear rates, the viscosity approaches a constant value, η_∞, which is insensitive to the clay concentration and decreases with the increasing repulsive interaction between the faces of the platelets.

For clay suspensions, clay platelets form micrometer-sized aggregations, with sufficient connectivity to produce a network structure [10], the size of which is considered to be comparable to the gap of the plates of rheometer; therefore, this size effect needs to be taken into account. In rheological experiments using a rotational rheometer, a cone-plate geometry is often adopted, producing a constant shear rate. With such a geometry, the experiment is carried out at a fixed (minimum) gap, thus an investigation on the size effect of the testing geometry is rarely included. On the other hand, the boundary slip and shear inhomogeneity may cause the gap-dependent behavior if the rheological properties are measured by the parallel-plate geometry. Boundary slips are quite commonly observed for polymeric fluids [19–21]. Also, in the study of other complex fluid systems, Paredes *et al.* [22] find an obvious boundary slip for emulsions if the surface is hydrophilic; Jossic and Magnin [23] find the boundary slip for Carbopol gels which alters the calculated yield stress if it is determined by the Herschel–Bulkley model. For Laponite clay suspensions, Pignon *et al.* [24] observe a

a)Author to whom correspondence should be addressed; electronic mail: arwang@zju.edu.cn

shear banding at low shear rates following yielding, while neither shear banding nor boundary slip is observed at medium to high shear rate. The gap-dependent behavior originated from the slip condition as well as shear inhomogeneity needs to be investigated for clay systems.

In this study, with the adoption of a parallel-plate geometry, the change of the rheological behavior of the bentonite suspension with the gap is investigated at both the gel and flowing states. From the experiment, the size effect of the testing geometry on the rheological behavior, the boundary slip, and the shear inhomogeneity is examined.

II. EXPERIMENT

A commercial sodium bentonite clay (Hongruitai Bentonite Technology Co., Ltd., China) is adopted. The moisture content is 12.5%, and the composition is shown in Table I. The bentonite clay is mixed homogeneously with the de-ionized water to produce samples with an overhead stirrer. The mixing time is 30 min, after which the mixed suspensions are allowed to rest for 24 h before measurements. The natural *p*H of the suspensions is around 9.5. The ionic strength is ~0.05M NaCl.

A DHR-1 rotational rheometer from TA Instrument is used in the rheological measurement, with a 25 mm diameter parallel-plate geometry. The average roughness of the default plate (smooth plate) is 0.143 μm. After a preshearing with $\dot{\gamma} = 1000\,s^{-1}$ and a shearing time of 30 s are applied, the sample is allowed to rest for 3 min prior to the viscometric test. Both the stress-control and shear-rate-control modes are adopted in the test in order to investigate the behavior at both the gel and flowing states. The shearing time before the data point is recorded at each shear step is 6 s. An equilibrium state can be reached at the shearing duration of 5 s for the 15 wt. % bentonite suspension at the flowing state. In the small amplitude oscillatory shear (SAOS) experiment, since shear stress is the key parameter controlling the yield behavior of clay suspensions, the control-stress mode is adopted with a stress amplitude of 10 Pa, which is well below the yield stress (~70 Pa). Therefore, the tests are all in the linear viscoelastic range. The temperature is kept at 25 °C. The gap-dependent behavior is investigated by a series of tests, in which the gap between the parallel-plate geometry, H, first increases from 200 to 1400 μm in sequence with an increment of 200 μm. The tests with increasing H are then followed by the tests with H decreasing from 1400 to 200 μm to complete one testing series. At least two such series of measurement are carried out in order to confirm the reproductivity of the phenomenon. The sample is used only once and discarded with a testing time of about 15 min to minimize errors caused by water evaporation from the suspension.

TABLE I. Composition of the bentonite clay used in the experiment.

Component	SiO_2 (%)	Al_2O_3 (%)	Fe_2O_3 (%)	CaO (%)	MgO (%)	K_2O (%)	Na_2O (%)	Loss on ignition (%)
Mass fraction	60.77	17.11	2.26	0.15	0.78	3.85	0.33	5.85

III. RESULTS

A. Gap-dependent behavior with smooth plates

The shear rate versus shear stress curves for the bentonite suspension at 15 wt. % concentration is shown in Fig. 1(a) under the stress-control mode. H is changed from 200 to 1400 μm. Obviously, a yield behavior can be observed. Similar to our previous studies [12,17], the yield stress, τ_y, is defined as the stress where the shear rate starts to increase significantly [more than 3 orders of magnitude as shown in Fig. 1(a)]. Before yielding, the suspension behaves in a solid-like behavior (i.e., deformation of the gel). After yielding, a significant shear thinning behavior is seen with increasing shear stress (Fig. 2). The shear thinning behavior is proposed to be due to the orientation and alignment of the clay platelets along with the flow [2,25].

Furthermore, Fig. 1(a) shows a notable change of the shear rate versus shear stress curves with the gap variation. This gap-dependent behavior can be found both at the yield point ($\tau = \tau_y$) and at the flowing state ($\tau \gg \tau_y$). At yielding, with increasing gap, there is a decreasing trend of τ_y as shown in Fig. 1(b). On the other hand, as shown in Fig. 1(a),

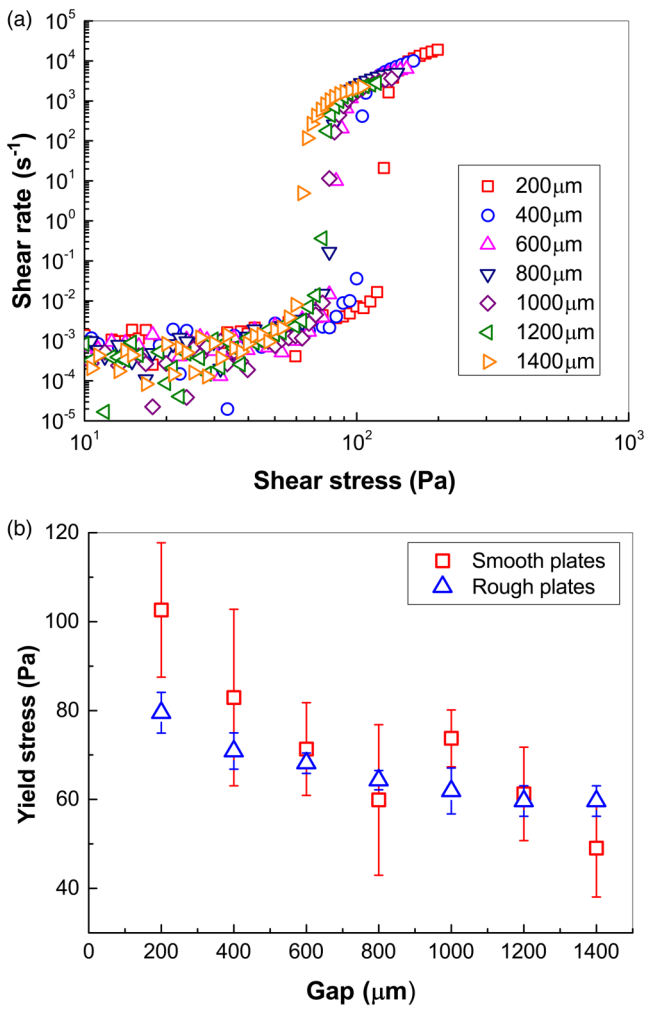

FIG. 1. (a) Shear rate as a function of shear stress at different gaps in the stress-control mode with smooth plates and (b) yield stress as a function of the gap for the 15 wt. % bentonite suspension with both the smooth and rough plates.

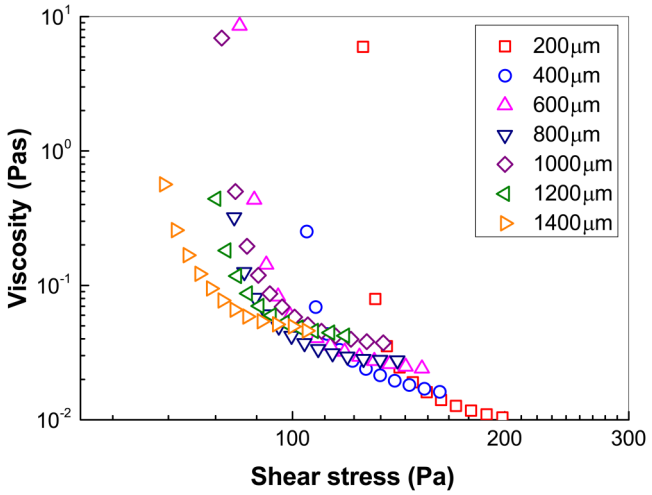

FIG. 2. Apparent viscosity as a function of shear stress at different gaps in the stress-control mode for the 15 wt. % bentonite suspension.

in a flow with high apparent shear rate ($\dot{\gamma}_a > 100\,\mathrm{s}^{-1}$), after the steep increase of the shear rate, the gap-dependent behavior can be observed as well. Sample loss at the edge of the plate is found in the experiment at high shear rates, the onset of which shifts to lower stress with increasing H. If the loss of sample occurs, $\dot{\gamma}_a$ measured increases abruptly, which quickly exceeds the maximum measurable value of the rheometer (not presented here). Curves of the apparent viscosity after yielding are shown in Fig. 2. The viscosity decreases with increasing stress, approaching a constant value, η_∞. Because of the sample loss at the edge, η_∞ at high stress cannot be achieved at small gaps. Also, it is difficult to compare all the viscosity data at a same shear stress since the onset of sample loss shifts toward low shear rates (stress) with increasing gap. However, the increasing trend of the constant viscosity at high stress with increasing H can still be deduced according to Fig. 2.

On the other hand, shear-rate-control experiments are also carried out as shown in Fig. 3. At a low shear-rate range

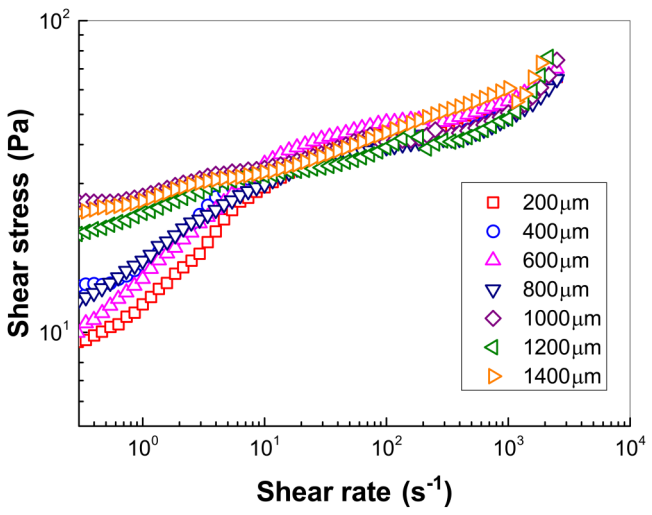

FIG. 3. Shear stress as a function of shear rate at different gaps in the shear-rate-control mode for the 15 wt. % bentonite suspension.

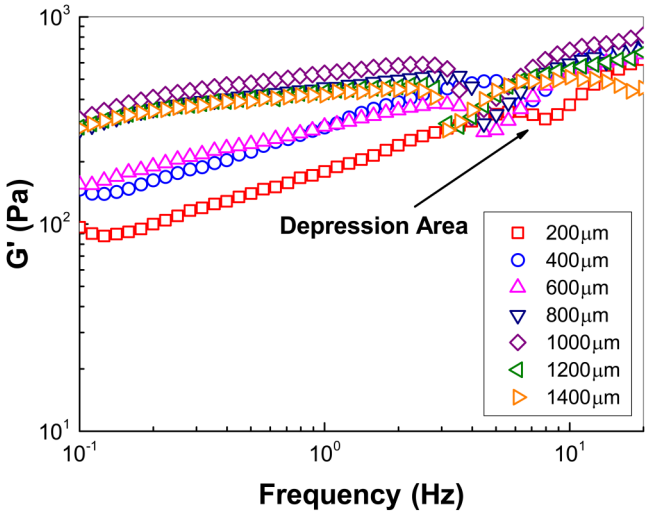

FIG. 4. Storage modulus as a function of frequency at different gaps in the small amplitude oscillatory shear experiment for the 15 wt. % bentonite suspension.

($\dot{\gamma}_a < 20\,\mathrm{s}^{-1}$), at a given shear rate, the shear stress increases with increasing H. When $H \geq 1000\,\mu$m, the increasing of stress with H becomes less obvious. The slope of the curves at $\dot{\gamma}_a < 20\,\mathrm{s}^{-1}$ decreases with increasing H, showing that the exponent, n_1, of the power-law behavior, $\tau \sim \dot{\gamma}^{n_1}$, at this range decreases with H, which indicates a more significant shear thinning with increasing H. With $\dot{\gamma}_a > 20\,\mathrm{s}^{-1}$, no obvious trend in the data with H can be observed for the shear-rate range examined ($\dot{\gamma}_a < 2000\,\mathrm{s}^{-1}$).

In order to analyze any possible change of the gel structure with H, a frequency sweep test in SAOS is carried out at different H as shown in Fig. 4. It is found that the storage modulus, G', is also very sensitive to changing of the gap. At low frequency, G' increases with increasing H. With $H \geq 800\,\mu$m, G' becomes insensitive to H. Furthermore, as shown in Fig. 4, a "depression" area can be observed at a frequency between 1 and 10 Hz, the location of which shifts toward lower frequency with increasing H.

B. Gap-dependent behavior with rough plates

For the purpose of identifying the effect of slippage on the experimental results, we further test the clay suspension with both the upper and lower plates of the rheometer covered by a glass paper of average roughness 11.3 μm. With these rough plates, the results are shown in Figs. 5–7. Compared to those obtained with the default plates (smooth plates, with a roughness of 0.143 μm), it can be found that the gap-dependent behavior is changed by the roughness. As shown in Fig. 1(b), the decreasing trend of τ_y with increasing H, determined from Fig. 5(a), can be observed for rough plates. The gap-dependent behavior of τ_y becomes less obvious compared to the one using smooth plates. At $\dot{\gamma} > 100\,\mathrm{s}^{-1}$, after the steep increase of the shear rate, it can be found that the shift of the shear rate curve with H is similar to Fig. 1(a). The behavior can be seen more clearly by the apparent viscosity as shown in Fig. 5(b). It can be deduced that the constant viscosity, η_∞, increases with

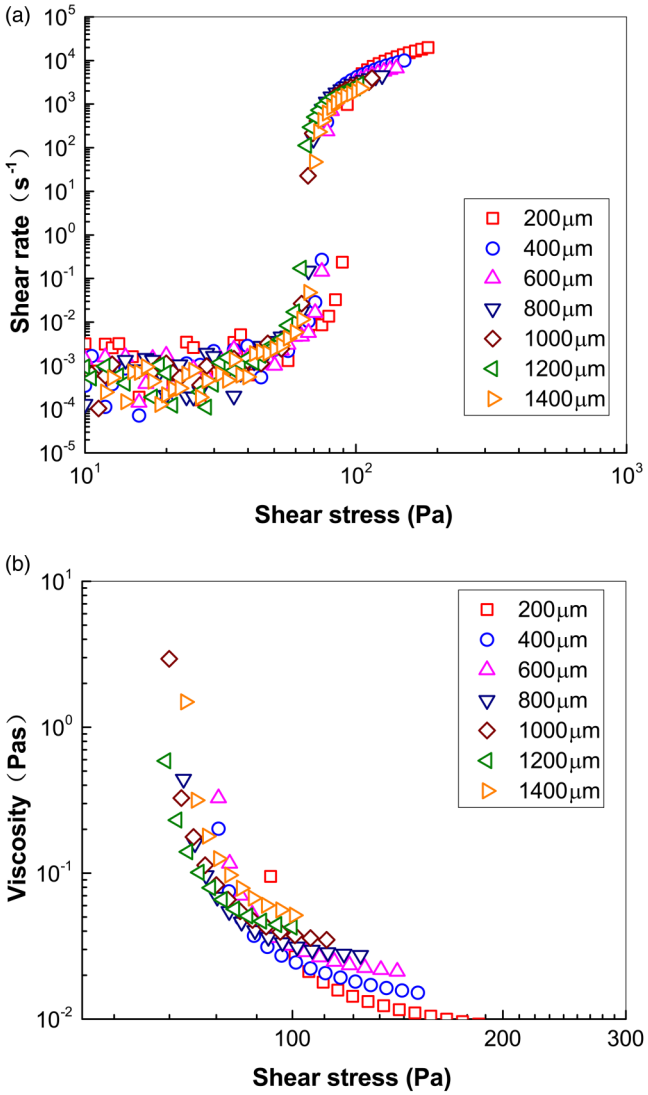

FIG. 5. (a) Shear rate and (b) apparent viscosity as a function of shear stress at different gaps in the stress-control mode. The parallel-plate geometry is covered by the glass paper (a roughness of 11.3 μm).

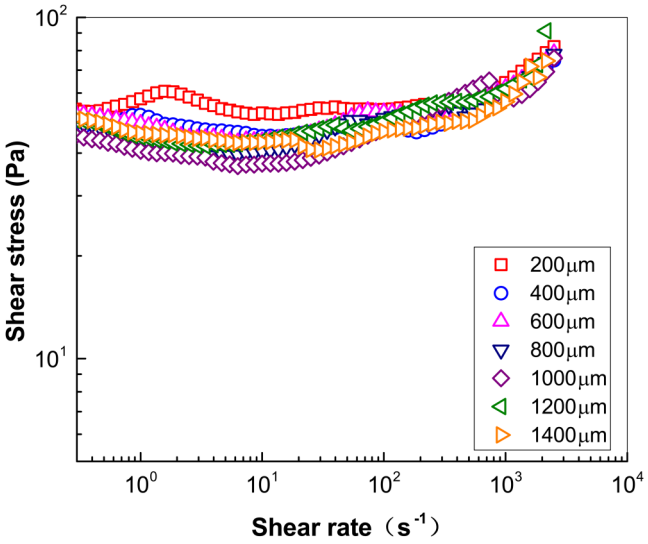

FIG. 6. Shear stress as a function of shear rate at different gaps in the shear-rate-control mode. The rheometer plates are covered by the glass paper (a roughness of 11.3 μm).

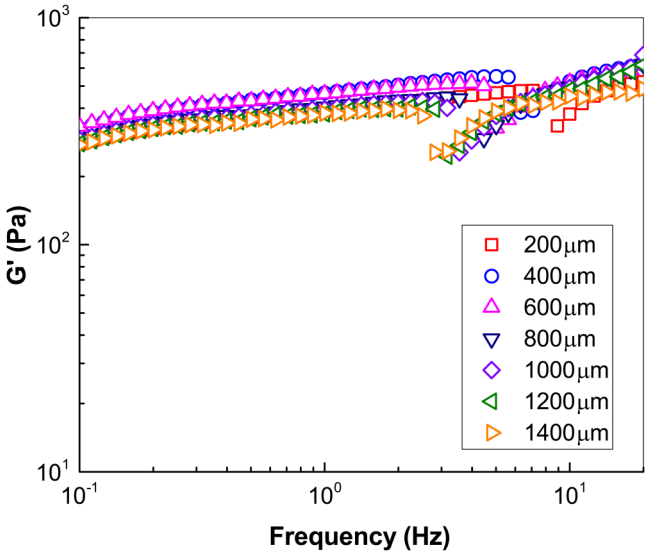

FIG. 7. Storage modulus as a function of frequency at different gaps in the small amplitude oscillatory shear experiment. The rheometer plates are covered by the glass paper (a roughness of 0.143 μm).

increasing H, which is similar to the behavior using smooth plates (Fig. 2).

The viscometric test under the shear-rate control mode is shown in Fig. 6. At a low shear-rate range ($\dot{\gamma}_a < 20\,\mathrm{s}^{-1}$), the dependence on H is distinct from Fig. 3 for smooth plates. The power-law behavior of the shear stress at low shear rates, $\tau \sim \dot{\gamma}^{n_1}$, is insensitive to H, i.e., $n_1 \approx 0$ for all gaps. The stress is nearly constant with $\dot{\gamma}$, approaching a constant value of τ_0. With increasing H, τ_0 first decreases and becomes relatively stable when $H \geq 800\,\mu$m. The evolution is similar to τ_y shown in Fig. 1(b) for rough plates. Also, τ_0 is larger than the shear stress measured with smooth plates at the same shear-rate range. It may be found that τ_0 is close to τ_y. Similar behavior can be observed for carbopol gels measured by smooth and rough testing plates, which is attributed to the slip at the fluid-tool interface [23]. With $\dot{\gamma}_a > 20\,\mathrm{s}^{-1}$, the curves seem to merge.

Results of the SAOS experiment with rough plates are shown in Fig. 7. The gap-dependent behavior is largely suppressed when the roughness is increased. Nevertheless, the shift of the depression area can still be observed with the location shifting toward lower frequency with increasing H, which is similar to the SAOS test by smooth plates.

IV. DISCUSSION

A. Slip and shear inhomogeneity at yielding

As shown in Fig. 1(b), when the system yields to flow, the yield stress, τ_y, decreases with increasing gap. Slip and/or shear banding are usually considered to result in the gap-dependent rheological behavior with the parallel-plate geometry. A monotonic change in the rheological properties with the gap is often observed if slippage at the boundary takes place, as shown in Fig. 8(b), which has been often discussed on polymeric solutions and melts [19,20,26]. With the boundary slip, according to Yoshimura and Prud'homme [20], the relation between the apparent shear rate measured by the rheometer, $\dot{\gamma}_a$, and the real

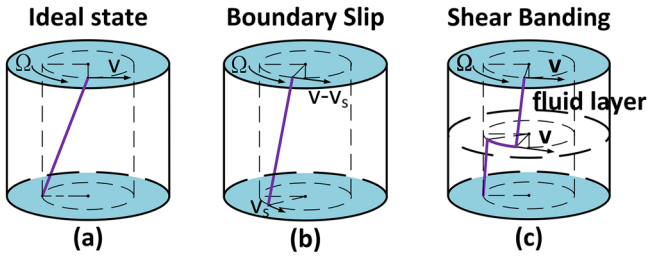

FIG. 8. Diagram of (a) ideal state (with no wall slip or shear inhomogeneity), (b) wall slip, and (c) shear banding in the rheological experiment on bentonite suspensions.

shear rate, $\dot{\gamma}_r$, can be written as

$$\dot{\gamma}_a = \dot{\gamma}_r(\tau) + \frac{2V_s}{H}, \tag{1}$$

where V_s is the slip velocity at the boundary. From Eq. (1), $\dot{\gamma}_r$ may be calculated as

$$\dot{\gamma}_r(\tau) = \frac{H_1\dot{\gamma}_{a1} - H_2\dot{\gamma}_{a2}}{H_1 - H_2}, \tag{2}$$

where $\dot{\gamma}_{a1}$ and $\dot{\gamma}_{a2}$ are apparent shear rates at gaps of H_1 and H_2, respectively. From Eq. (1), it can be deduced that $\dot{\gamma}_a$ decreases, approaching $\dot{\gamma}_r$ with increasing H. As shown in Fig. 5, it seems that the change of yield behavior on H still exists when using rough plates. Therefore, the gap-dependent behavior at yielding is not attributable to the slip at the boundary.

As observed by Pignon *et al.* [24] for Laponite suspensions, when the sample yields to flow, shear banding occurs, in which the yielding is first located within a thin layer of the sample. In this case, the sample between the measuring plates is formed by a uniform fluid layer sandwiched between two elastically deformed solid bands as shown in Fig. 8(c). The thickness of the fluid layer then increases with increasing $\dot{\gamma}_a$. Thus, at the yielding point, the shearing occurs practically in the layer, while the sample in upper and lower solid bands can be regarded as parts of the upper and lower plate, respectively. For the parallel-plate geometry, the apparent shear rate is calculated as

$$\dot{\gamma}_a = \Omega\frac{r}{H}, \tag{3}$$

where Ω is the angular velocity and r is the radial position in the sample. Therefore, the real shear rate in the layer is estimated as

$$\dot{\gamma}_r = \Omega\frac{r}{e} = \dot{\gamma}_a\frac{H}{e}, \tag{4}$$

where e is the thickness of the shearing layer and is considered to be independent of H.

If we consider the shear banding as the cause for the changing of τ_y with H, at the vicinity of yielding point, e.g., $\dot{\gamma}_a = 0.1\,\mathrm{s}^{-1}$, from Eq. (4), we can deduce that $\dot{\gamma}_r$ increases with increasing H. Since τ should increase with increasing $\dot{\gamma}$ in the stress-control mode according to the curves shown in Fig. 5, for example, τ increases with increasing H at the vicinity of yielding, which is not consistent with the experimental data in Fig. 1 or 5 (τ deceases with increasing H as is identical to the behavior of τ_y).

Consequently, from the discussion above, we may conclude that the decrease of τ_y with increasing H is due to neither the boundary slip nor the shear banding.

B. Slip and shear inhomogeneity at low shear rates

Comparing the results shown in Figs. 3 and 6, it can be deduced that the surface roughness affects the rheological behavior measured for bentonite suspensions. Slippage takes place for bentonite suspensions at low shear rates when $\dot{\gamma} \leq 20\,\mathrm{s}^{-1}$, which causes a significant gap-dependent behavior in Fig. 3. From Eq. (1), it maybe deduced that the curve of $\dot{\gamma}_a$ approaches asymptotically to the curve of $\dot{\gamma}_r$ with increasing H. Therefore, at high H, it is excepted that $\dot{\gamma}_a$ should become less sensitive to the gap, which agrees with our experimental results at low shear rate (Fig. 3). It is found that the gap dependent behavior becomes less obvious with increasing $\dot{\gamma}_a$ and disappears when $\dot{\gamma}_a$ reaches a critical value of about $20\,\mathrm{s}^{-1}$. Less boundary slip with increasing $\dot{\gamma}_a$ should be responsible for the changing of the power-law behavior n_1 in $\tau_0 \sim \dot{\gamma}^{n_1}$ with increasing H (n_1 decreases with increasing H) in Fig. 3. With $\dot{\gamma}_a > 20^{-1}$, it thus can be deduced that slip vanishes and $\dot{\gamma}_a = \dot{\gamma}_r$. This finding is close to the result of Pignon *et al.* [10]. They find a critical value of $10\,\mathrm{s}^{-1}$, above which the Laponite suspension is sheared homogeneously throughout the gap.

It is noted in Fig. 6 that with rough plates, $n_1 \approx 0$, indicating a shear banding according to Pignon *et al.* [24], who find shear banding for Laponite suspensions at low shear. In this case, the sample between the measuring plates is formed by a uniformly fluid band sandwiched between two elastically deformed solid bands. Shear inhomogeneity is a consequence of the yielding that is similar to the localized yielding in entangled polymers [27]. The thickness of the fluid band increases with increasing $\dot{\gamma}_a$, while τ remains constant ($n_1 \approx 0$) until the fluid band extends across the entire gap between the plates. Interestingly, it may be proposed from our results that, shear banding disappears when the boundary slip takes place, because as shown in Fig. 3 when slip takes place, $n_1 > 0$ for the power-law behavior at the same $\dot{\gamma}_a$ range. Finally, with $\dot{\gamma}_a > 20\,\mathrm{s}^{-1}$, the curves for both smooth and rough plates approaches each other, indicating that the sample is correctly entrained and deformed throughout the gap in the shear-rate range of $20–1000\,\mathrm{s}^{-1}$.

In order to confirm the slip and banding at a low shear rate for smooth and rough plates, respectively, we apply an optical observation simply by marking a straight line vertically at the edge of the sample, connecting the upper and lower plates ($H = 2000\,\mu\mathrm{m}$). The flow condition across the edge of the sample is evaluated at a shear rate of $2\,\mathrm{s}^{-1}$ and a shearing time of 3 s (i.e., with the strain of 6), by the deformation of the line. As shown in Fig. 9, the slip at the boundary when using smooth plates [Fig. 9(a)] as well as the shear banding using rough plates [Fig. 9(b)] can be identified, which confirms our deduction from the rheological experiments.

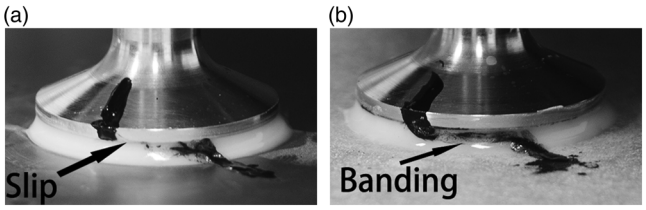

FIG. 9. Boundary slip and shear banding observed using the (a) smooth and (b) rough plates, respectively, at the shear rate of $2\,s^{-1}$ and a shearing time of 3 s. The gap between the plates is $2000\,\mu m$. The upper plate rotates in the clockwise direction.

Furthermore, at $\dot{\gamma}_a < 20\,s^{-1}$, the stress with rough plates, τ_0, seems to decrease with increasing H and becomes insensitive to H when $H > 800\,\mu m$, similar to the behavior of τ_y with H [as shown in Figs. 1(b) and 5(a)]. In fact, τ_0 is identical to a yield stress determined by the Herschel-Bulkey model. Considering that τ_0 is close to τ_y, we may propose that the gap-dependent behavior of τ_0 has the same origin as the behavior at the yielding point, which should be connected to the change in the structure of the sample with the gap.

C. Slip and shear inhomogeneity in the SAOS experiment

As shown in Figs. 4 and 7, the changing of G' with H at low frequency disappears when rough plates are adopted, meaning that the boundary slip plays an important role in the SAOS experiment. On the other hand, a depression area can be observed at the frequency between 1 and 10 Hz. The location of such area shifts toward lower frequency with increasing H, regardless of the roughness changed. Clearly, the boundary slip is not responsible for this phenomenon.

D. Slip and shear inhomogeneity at high shear rates

With $\dot{\gamma}_a > 1000\,s^{-1}$, it can be found that the shear thinning is reduced, and a constant viscosity, η_∞ is approached [see Figs. 1(a), 2, and 5]. Pignon *et al.* [10] observe the deformation and disaggregation of the gel structure from the microscale to the nanoscale range with increasing shear. Philippe *et al.* [25] find that at high shear rates, the clay plates form layers along with the stream lines, which reduces the influence of the clay concentration, i.e., the viscosity at high shear rate, η_∞, becomes insensitive to the mass fraction. From Figs. 2 and 5(b), it can be discovered that the curve shifts monotonically, and η_∞ increases with increasing H. This behavior is not affected by the roughness. Therefore, the slip at the boundary should not be accountable for the shifting of the curve with the gap. Pignon *et al.* [10,24] also find experimentally that neither slip nor shear inhomogeneity is observed at high shear rates for Laponite suspensions. Since it is considered that, with $\dot{\gamma}_a$ approaching $O(10^4)\,s^{-1}$, the structure is layers formed by clay platelets aligning with flow. It may be that the platelets can be better aligned at small H due to the confinement by the upper and lower plates, which increases the fluidity. This is similar to the cooperative effects for emulsion systems observed by Paredes *et al.* [22]. Cooperative effects are caused by the local rearrangement of the suspending phase, which is due to the confining effect by the testing geometry. With the cooperative effects, the viscosity decreases with decreasing H, which can be treated as an effective boundary slip.

E. Size effect on the structure

Other than the boundary slip and shear inhomogeneity, it can be found that the size of the testing geometry does affect the gel structure of bentonite suspensions at both the gel and flowing states. As is similar to the relaxation for polymeric systems, we considered that clay suspension systems also have time dependent feature reflecting a certain motion of the network structure in the gel. The depression area in Figs. 4 and 7 thus indicates a fluctuation of the structure of a certain scale (e.g., in the microscale range) in the gel system. It is found that locations of the depression area shift to a lower frequency, indicative of a slower motion of such structure with increasing H. As shown in Fig. 10, from the location of the depression area, we can deduce "characteristic relaxation times," $\lambda = \omega^{-1}$, at different gaps for the tests using both smooth and rough plates. λ is insensitive to the roughness of plates. Approximately, $\lambda \propto H$.

At the gel and flowing states with low shear rates, the mesoscale structure of the bentonite suspension may be clusters of platelets of nanoscales with the face-face or face-edge configuration, according to the repulsive or attractive interactions, respectively [12,18]. At larger length scales, Pignon *et al.* [10] find that the micrometer-sized aggregates are rearranged to form a continuous three-dimensional structure. Gelation is formed by such a continuous structure which should have the overall length scale determined by the testing geometry. Therefore, the length scale increases with increasing gap and results in a slower "relaxation behavior" of the structure at higher H.

The yielding in the shearing layer, reflected by τ_y as well as τ_0 at low shear rates as discussed in Secs. IV A and IV B, should be largely influenced by the length scale of the network structure, which seems decreases with the increasing size of the structure. In bentonite suspensions, it is proposed that the yield behavior is due to the deformation of the gel

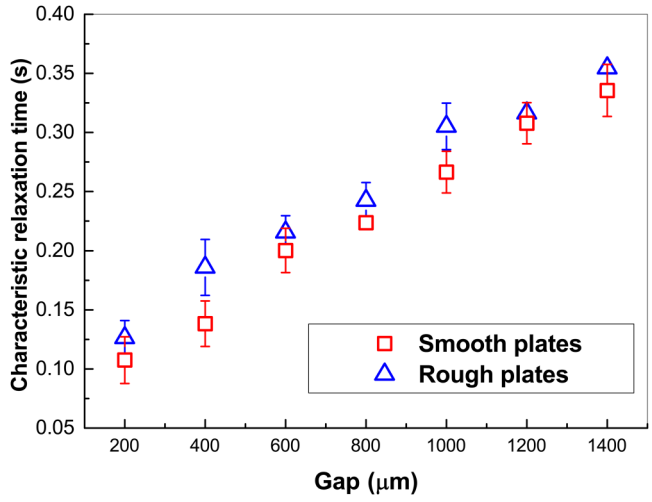

FIG. 10. Change of the characteristic relaxation time with the gap deduced from the small amplitude oscillatory shear experiment for the 15 wt. % bentonite suspension.

structure that is stabilized by the nanoscaled face-to-face repulsive electrostatic interactions between bentonite platelets [12], the strength of which increases with increasing concentration. Therefore, we may regard that the strength of the electrostatic interparticle interactions is not changed if the mass fraction of clay is determined. Nevertheless, the network across the gap of the plates may be considered as the connectivity between the upper and lower plates, the length of which thus increases with increasing H. The thicker the network, the easier it is fractured. This may explain the decrease of τ_y and τ_0 with increasing H.

V. CONCLUSION

From rheological experiments on bentonite suspensions using a rheometer with the parallel-plate geometry at different gaps, it is found that (1) boundary slip plays an important role both at a low shear-rate range ($\dot{\gamma}_a < 20\,\mathrm{s}^{-1}$, in a shear-rate-control mode) and in the SAOS experiment; (2) shear banding occurs both at the vicinity of the yielding point in the stress-control mode and at a low shear-rate range ($\dot{\gamma}_a < 20\,\mathrm{s}^{-1}$) when the boundary slip is suppressed by roughed plates in a shear-rate-control mode; and (3) the size of the network structure increases with increasing testing geometry (i.e., the gap), which results in a decrease of the yield stress, as well as the stress at low shear rate range, with increasing gap.

ACKNOWLEDGMENTS

This study is supported by the National Natural Science Foundation of China (NNSFC, No. 11702246), the National Key R&D Program of China (Grant No. 2017YFC0307703), and the Fundamental Research Funds for the Central Universities (No. 2018FZA4022).

REFERENCES

[1] Zhang, F., W. Zhang, X. Zhang, X. Feng, L. Lin, K. Zhu, K. Chen, Y. Meng, and X. Feng, "Key technique and scheme of classification and nomenclature for deep sea sediments," Earth Sci. J. China Univ. Geosci. **37**, 93–104 (2012).

[2] Paineau, E., L. J. Michot, I. Bihannic, and C. Baravian, "Aqueous suspensions of natural swelling clay minerals. 2. Rheological characterization," Langmuir **27**, 7806–7819 (2011).

[3] Michot, L. J., C. Baravian, I. Bihannic, S. Maddi, C. Moyne, J. F. Duval, P. Levitz, and P. Davidson, "Sol-gel and isotropic/nematic transitions in aqueous suspensions of natural nontronite clay. Influence of particle anisotropy. 2. Gel structure and mechanical properties," Langmuir **25**, 127–139 (2008).

[4] Cocard, S., J. F. Tassin, and T. Nicolai, "Dynamical mechanical properties of gelling colloidal disks," J. Rheol. **44**, 585–594 (2000).

[5] Coussot, P., Q. D. Nguyen, H. T. Huynh, and D. Bonn, "Viscosity bifurcation in thixotropic, yielding fluids," J. Rheol. **46**, 573–589 (2002).

[6] Abou, B., D. Bonn, and J. Meunier, "Nonlinear rheology of laponite suspensions under an external drive," J. Rheol. **47**, 979–988 (2003).

[7] Ferroir, T., H. T. Huynh, X. Chateau, and P. Coussot, "Motion of a solid object through a pasty (thixotropic) fluid," Phys. Fluids **16**, 594–601 (2004).

[8] Chafe, N. P., and J. D. Bruyn, "Drag and relaxation in a bentonite clay suspension," J. Nonnewton. Fluid Mech. **131**, 44–52 (2005).

[9] Adachi, Y., K. Nakaishi, and M. Tamaki, "Viscosity of a dilute suspension of sodium montmorillonite in a electrostatically stable condition," J. Colloid Interface Sci. **198**, 100–105 (1998).

[10] Pignon, F., A. Magnin, and J. M. Piau, "Thixotropic behavior of clay dispersions: Combinations of scattering and rheometric techniques," J. Rheol. **42**, 1349–1373 (1998).

[11] Baird, J., and J. Walz, "The effects of added nanoparticles on aqueous kaolinite suspensions: II. Rheological effects," J. Colloid Interface Sci. **306**, 411–420 (2007).

[12] Lin, Y., N. Phan-Thien, J. B. P. Lee, and B. C. Khoo, "Concentration dependence of yield stress and dynamic moduli of kaolinite suspensions," Langmuir **31**, 4791–4797 (2015).

[13] Laxton, P. B., and J. C. Berg, "Relating clay yield stress to colloidal parameters," J. Colloid Interface Sci. **296**, 749–755 (2006).

[14] Teh, E., Y. Leong, Y. Liu, A. Fourie, and M. Fahey, "Differences in the rheology and surface chemistry of Kaolin clay slurries: The source of the variations," Chem. Eng. Sci. **64**, 3817–3825 (2009).

[15] Leong, Y.-K., J. Teo, E. Teh, J. Smith, J. Widjaja, J.-X. Lee, A. Fourie, M. Fahey, and R. Chen, "Controlling attractive interparticle forces via small anionic and cationic additives in Kaolin clay slurries," Chem. Eng. Res. Des. **90**, 658–666 (2012).

[16] Sakairi, N., M. Kobayashi, and Y. Adachi, "Effects of salt concentration on the yield stress of sodium montmorillonite suspension," J. Colloid Interface Sci. **283**, 245–250 (2005).

[17] Lin, Y., L. K.-J. Cheah, N. Phan-Thien, and B. C. Khoo, "Effect of temperature on rheological behavior of kaolinite and bentonite suspensions," Colloids Surf. A Physicochem. Eng. Aspects **506**, 1–5 (2016).

[18] Leong, Y.-K., M. Du, P.-I. Au, P. Clode, and J. Liu, "Microstructure of sodium montmorillonite gels with long aging time scale," Langmuir **34**, 9673–9682 (2018).

[19] Lin, Y., and Y. Fan, "Slippage and shear inhomogeneity in shear-induced crystallization of isotactic polypropylene on metal substrates," Rheol. Acta **52**, 369–381 (2013).

[20] Yoshimura, A., and R. K. Prud'homme, "Wall slip corrections for Couette and parallel disk viscometers," J. Rheol. **32**, 53–67 (1988).

[21] Boukany, P. E., P. Tapadia, and S. Q. Wang, "Interfacial stick-slip transition in simple shear of entangled melts," J. Rheol. **50**, 641–654 (2006).

[22] Paredes, J., N. Shahidzadeh, and D. Bonn, "Wall slip and fluidity in emulsion flow," Phys. Rev. E **92**, 042313 (2015).

[23] Jossic, L., and A. Magnin, "Drag and stability of objects in a yield stress fluid," AIChE J. **47**, 2666–2672 (2001).

[24] Pignon, F., A. Magnin, and J. M. Piau, "Thixotropic colloidal suspensions and flow curves with minimum: Identification of flow regimes and rheometric consequences," J. Rheol. **40**, 573–587 (1996).

[25] Philippe, A. M., C. Baravian, M. Imperor-Clerc, S. J. De, E. Paineau, I. Bihannic, P. Davidson, F. Meneau, P. Levitz, and L. J. Michot, "Rheo-saxs investigation of shear-thinning behaviour of very anisometric repulsive disc-like clay suspensions," J. Phys. Condens. Matter **23**, 194112 (2011).

[26] Henson, D. J., and M. E. Mackay, "Effect of gap on the viscosity of monodisperse polystyrene melts: Slip effects," J. Rheol. **39**, 359–373 (1995).

[27] Wang, S. Q., S. Ravindranath, and P. E. Boukany, "Homogeneous shear, wall slip, and shear banding of entangled polymeric liquids in simple-shear rheometry: A roadmap of nonlinear rheology," Macromolecules **44**, 183–190 (2011).